Available online at www.sciencedirect.com
SCIENCE DIRECT®

Journal of the European Ceramic Society 23 (2003) 1617–1628
www.elsevier.com/locate/jeurceramsoc

Interactions between a leadless glaze and a biscuit fired bone china body during glost firing—part III: effect of glassy matrix phase

Alpagut Kara[a,*], Ron Stevens[b]

[a]Department of Materials Science and Engineering, Anadolu University, Eskisehir, Turkey
[b]Department of Engineering Science and Applied Science, University of Bath, Bath, UK

Received 15 June 2002; received in revised form 21 October 2002; accepted 2 November 2002

Abstract

As the final part of the study, the interactions between a commercial leadless glaze and a simulated bone china body glass during glost firing at different temperatures have been investigated. Advanced techniques such as electron probe microanalysis (EPMA) and transmission electron microscopy (TEM) have been employed in order to assess the contribution of the glassy phase of a biscuit fired bone china body to the formation of interaction layers at the interfaces independently. The results showed the presence of several calcium phosphate phases with distinct morphology at the glaze-simulated body glass interface for both the glost firing temperatures employed. It was suggested that the formation of the hydroxyapatite crystals at the glaze-biscuit fired bone china body interface may be helped by the glassy phase. TEM was found to be particularly useful since the interaction layers presented a most complicated and also interesting microstructure due in part to their multi-layered nature and small size of the calcium phosphate crystals situated at the interfaces.

Keywords: Bone china; Glazes; Glost firing; Hydroxyapatite; Interface; Tableware

1. Introduction

Earlier reports of this work have been limited to the preparation of the crystalline phases of a typical biscuit fired bone china body and the subsequent interface studies for simulating independently the interactions between an ABS type leadless glaze and the individual crystalline phases originally present in the body during glost firing at different temperatures.[1,2] With the combined use of XRD and SEM techniques in these studies, the presence of a range of interactions layers with distinctly different morphological and chemical characteristics was demonstrated. It was also proposed that β-TCP was the major contributor to the overall interactions, by reacting with CaO from the glaze in the presence of water vapour, and forming hydroxyapatite crystals at the glaze–body interfaces. In regard to the contribution of the glassy matrix phase, however, the inference was made that the glassy phase played a role by helping the formation of a low viscosity melt together with the glaze at higher temperatures hence increasing the mobility of the diffusing elements. It was also suggested that any free phosphorus ions present in the glassy matrix might react with CaO from the glaze. As a result, further work was suggested at the time in order to evaluate its contribution.

A recent study on the biscuit firing of a bone china body and the formation and the chemistry of its constituent phases was also carried out by the authors of this paper.[3,4] They successfully demonstrated that β-TCP, anorthite and a negligible amount of quartz were the only crystalline phases, all rather unevenly dispersed in a glassy matrix phase following firing at a peak temperature of 1245 °C for 1 h soaking. In addition, the glassy matrix phase was shown to have an inhomogeneous distribution and varying chemistry, in particular with different amounts of phosphorus; this was given as supportive evidence for the hypothesis

* Corresponding author. Tel.: +90-222-321-3550; fax: +90-222-323-9501.
E-mail address: akara@anadolu.edu.tr (A. Kara).

0955-2219/02/$ - see front matter © 2003 Elsevier Science Ltd. All rights reserved.
PII: S0955-2219(02)00403-X

associated with "the phosphate glass equation".[5] According to this hypothesis, the solid state reaction between bone ash and china clay releases P_2O_5, and this was postulated to become incorporated into the glassy phase with other of the body materials not taken up in the reaction. This result differs from earlier studies on the microstructural analysis of several commercial bone china bodies, where P_2O_5 was never detected in the glassy matrix.[6,7]

Of the different techniques used to examine the glaze–body interactions, the ideal for this type of study is EPMA. With EPMA, changes in chemical composition of both glaze and body in the vicinity of the interface and at considerable distances from it, can be detected, and if the two have reacted to form a layer of different composition, this can be analysed. The first use of EPMA for the study of the glaze–body interactions was reported by Ruddlesden and Airey[8] and Roberts and Marshall[9] over 30 years ago. Most of their work was based on obtaining X-ray line scans of the relevant elements across the glaze–body interfaces. It is worth mentioning that the present generation of dedicated microprobes are now much more sensitive. Further information can be obtained using of the TEM, the main advantage over other electron microscope techniques being that a high resolution investigation of the crystalline and glassy phases in the interaction layers can be achieved.

The present study was undertaken to assess the contribution of the glassy matrix phase to the overall formation of interaction layers between an ABS type commercial leadless glaze and a biscuit fired bone china body during glost firing at different temperatures.

2. Experimental

2.1. Material preparation

The simulated bone china body glass employed in this study was the one suggested by Roberts and Beech[5] based on "the phosphate glass equation" and later used by Roberts and Marshall[9] in one of the most comprehensive work for the study of glaze-body interactions. As mentioned above, the same glass composition was also prepared and studied previously by the present authors in order to compare its structure and chemistry with that of the glassy phase originally present in a biscuit fired bone china body.[4] Necessary details concerning the composition and the preparation of this glass can be found in that paper. In addition, the preparation of the glaze slip, its application onto the polished surfaces of the simulated body glass samples and the glost firings (1060 and 1120 °C) were achieved in the same manner described in the second part of the study.[2]

2.2. Techniques

In addition to XRD and SEM techniques, EPMA and TEM have also been employed in order to assess the interactions between the ABS glaze and the simulated bone china body glass during glost firing. EPMA studies were achieved on the polished cross-section of the ABS glaze-simulated body glass interface with a JEOL JXA-8600 superprobe electron probe microanalyser. Representative specimens were coated with carbon before the analyses. The coating unit was Model 12E6, Edwards High Vacuum Ltd., England. The elemental distribution profiles were obtained across the underlying body glass, interface and the glaze layer to follow up the variations of oxide contents, using four computer controlled WDS spectrometers. This was accomplished mainly by moving the sample in 1 μm intervals under an approximately 1 μm stationary electron beam and taking X-ray counts at each interval (line scan). Characteristic X-ray counts of relevant elements were collected through the microanalysis time of 10 s for each interval. The electron accelerating voltage and the beam current were 10 kV and $\sim 7.4\times10^{-8}$ μA, respectively. No quantitative analysis was attempted due to the number of elements and the complex nature of the interfaces involved.

The procedure in order to prepare the cross-sectional TEM specimen of the glaze–simulated body glass interface was developed from the published techniques for the examination of coatings.[10] For this, two glazed pieces are glued together with the glazed surfaces face to face using standard twin pack Araldite. The configuration was then clamped together until the Araldite had cured. The resulting sandwich was then ground down to such dimensions, on the SiC papers, by hand, that it would fit and could be glued into a brass tube of 3 mm external diameter and 2 mm internal diameter. The assembly was then sectioned into about 300–400 μm thick slices with a diamond wafering blade on a precision saw. A representative slice was then mounted on a glass slide with quartz wax and ground and polished until a level and polished surface was achieved with a thickness of around 100 μm. Finally, the cross-sectional TEM specimen was mechanically dimpled on both sides using a dimpler, model: D500i, (VCR Group Inc., USA) and thinned by ion beam milling to electron transparency using argon from both sides simultaneously, at room temperature, on a Gatan dual ion mill thinner, model 600 (England). Coating of the specimen, in order to ensure specimen stability in the electron beam, was achieved with a thin layer of carbon (Model: 12E6, Edwards High Vacuum Ltd., England) prior to TEM observation.

TEM studies were performed using a JEOL 200 kV analytical electron microscope using a side entry, single tilt holder. The morphology of crystalline and vitreous phases present at the interface were examined in detail.

Chemical microanalyses of the phases were obtained using the EDS attachment, an Oxford Instruments AN 10/25 Link microanalysis system, mounted without a window, allowing light elements such as sodium and oxygen to be analysed without difficulty. All images and EDS spectra were recorded using a 200 kV incident electron beam.

Note that XRD, EPMA and TEM studies were only achieved on the representative samples glost fired at 1120 °C due to the similar nature of the interaction layers for both glost firing temperatures.

3. Results and discussion

3.1. SEM results

SEM examination of the polished cross-sections of ABS glaze–simulated body glass interfaces revealed a complicated interaction layer formation at both glost firing temperatures. Figs. 1(a) and (b) illustrate typical BE images of such interfaces fired at 1060 and 1120 °C respectively. There is sufficient atomic number contrast present to appreciate that the interaction layer was

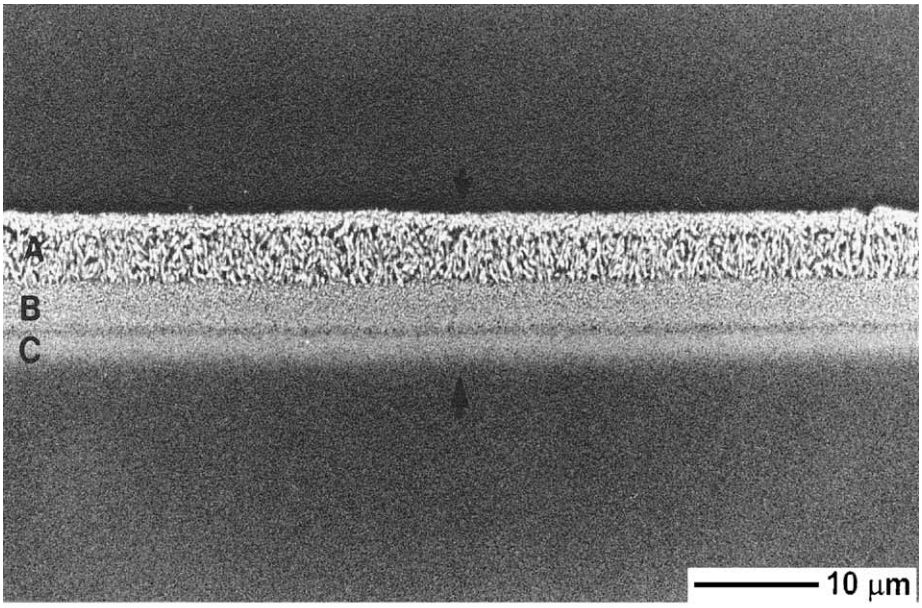

(a) glost fired at 1060°C

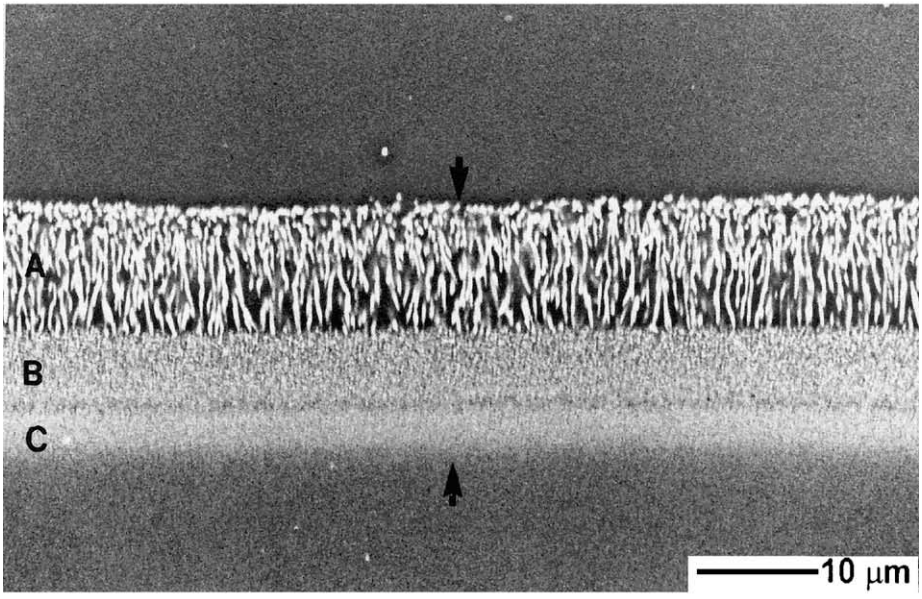

(b) glost fired at 1120°C

Fig. 1. Typical BE images of the polished cross-sections of the ABS glaze–simulated bone china body glass interface.

actually made up of at least three distinct continuous layers (designated as A, B, C). It is apparent in Fig. 1(b) that the white top layer close to the glaze (layer A) consists of acicular crystals having unidirectional growth into the glaze layer. The layer B also shows features of crystallinity but it was difficult to resolve individual crystals, even when higher magnifications were employed. The layer C in contact with the body glass itself, however, appears to be glassy in nature. Finally, there appears to be another glassy layer with a thickness of about 0.5 μm between B and C. The bright nature of the whole interaction layer in comparison with the glaze and the body glass is considered as an indication of the presence of high atomic number elements. An almost two fold increase in the thickness of the whole interaction layer (marked with arrows) with an increase of 60 °C in the glost firing temperature is evident from the images. Note that as opposed to the interaction layers between the glaze and the experimental crystalline phases of the bone china body, no etching procedure was developed for the glaze–simulated bone china body glass interfaces.

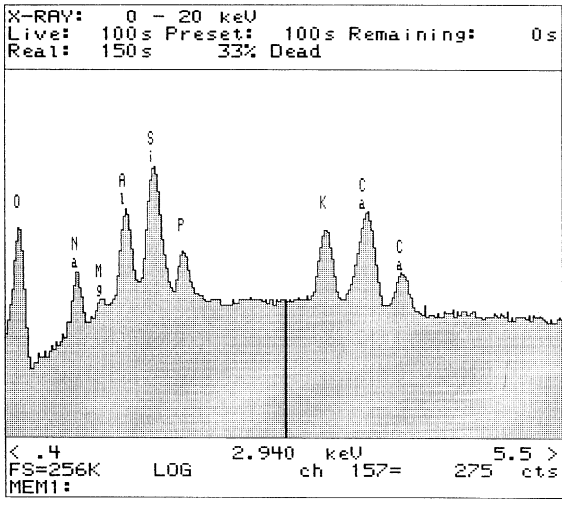

Fig. 2. A typical EDS spectrum of layer A.

EDS analyses were carried out on the layer A in order to understand the general chemistry of the interaction layer. Fig. 2 is a typical EDS spectrum from the layer A shown in Fig. 1 (b). The presence of P and Ca in the spectrum suggests that P present in the body glass probably reacts with Ca in the glaze to form a calcium phosphate based compound.

Fig. 3 is a typical BE image of the polished top surface (layer A) of the ABS glaze-simulated bone china body glass interface. The areas with high contrast are believed to represent the end-sections of acicular crystals grown almost perpendicular to the glaze. Note that this image was taken from the same surface whose XRD spectrum is given in Fig. 6.

3.2. EPMA results

The main problem encountered in the course of the EPMA studies of the interfaces was the behaviour of alkali elements, namely Na and K, in the glaze and the simulated body glass under the electron beam. An initial decrease in X-ray intensities of Na and K was observed under the operating conditions of the microprobe given above. Compositional changes in glazes and glasses during electron bombardment for electron microprobe analysis were also reported by several investigators.[11–13] While the nature of the compositional change depends strongly on the composition of the glass, the effect has

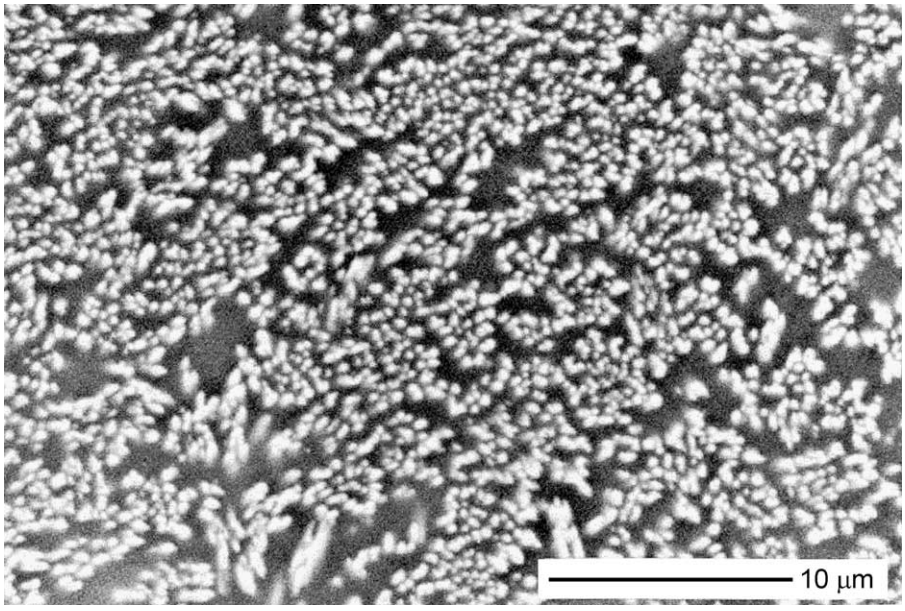

Fig. 3. A typical BE image of the ABS glaze–simulated bone china body glass interface glost fired at 1120 °C (polished top surface).

been most pronounced for glasses containing alkalis. The mechanisms that were proposed for explaining the alkali decay effects in various glasses are volatilisation,[14] desorption,[15] surface damage[16] and diffusion and ion migration.[16–19] Several methods have been suggested to deal with the problem of alkali decay effects during the EPMA analyses of glasses and glass-ceramics.[11–13,20] The results of individual procedures are accumulative so that an optimum analytical scheme will incorporate as many of the individual steps as possible.

The main technique employed in this study in order to deal with the problem of the decay of Na and K in the specimens was to scan a band of about 50 μm wide by 1 μm thick with the electron beam oriented parallel to the interface, thus distributing the time-average intensity of the beam over an area large enough to produce negligible alkali decay. In addition, the mean beam current was reduced to 1×10^{-8} μA as compared to 7.4×10^{-8} μA since large currents lead to greater specimen damage. The accelerating voltage, the microanalysis time, and the step size remained unchanged. The net result of these procedures was the reduction of the alkali decay observed at the beginning of the EPMA work to negligible levels.

Fig. 4 gives the typical elemental distribution profiles obtained from the polished cross-section of the ABS glaze–simulated bone china body glass interface, glost fired at 1120 °C. Note that the right-hand side of all the profiles is the glaze layer with a thickness of around 120–130 μm, the left-hand side is the underlying glass.

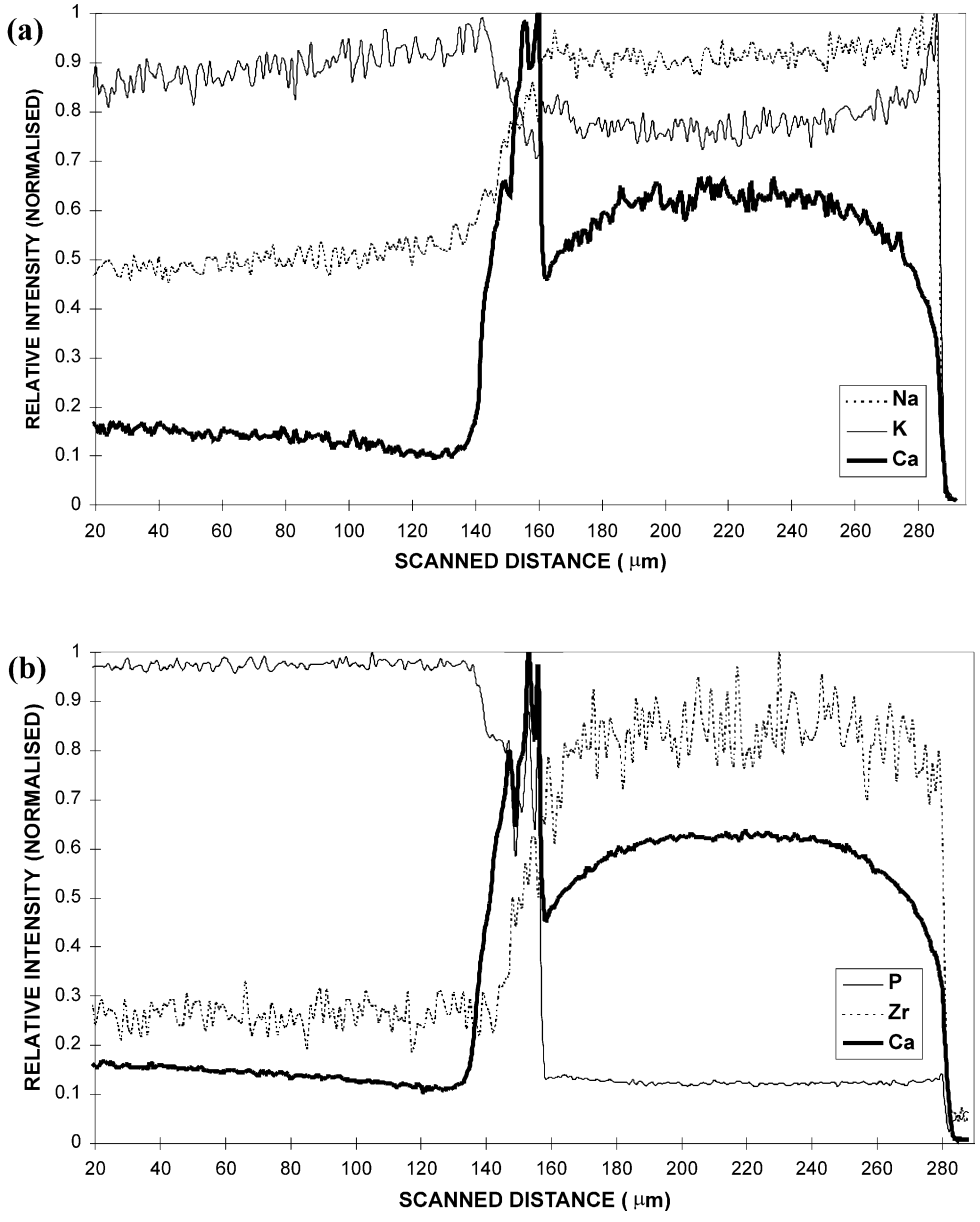

Fig. 4. The EPMA elemental distribution profiles across the ABS glaze–simulated bone china body glass interface (glost fired at 1120 °C).

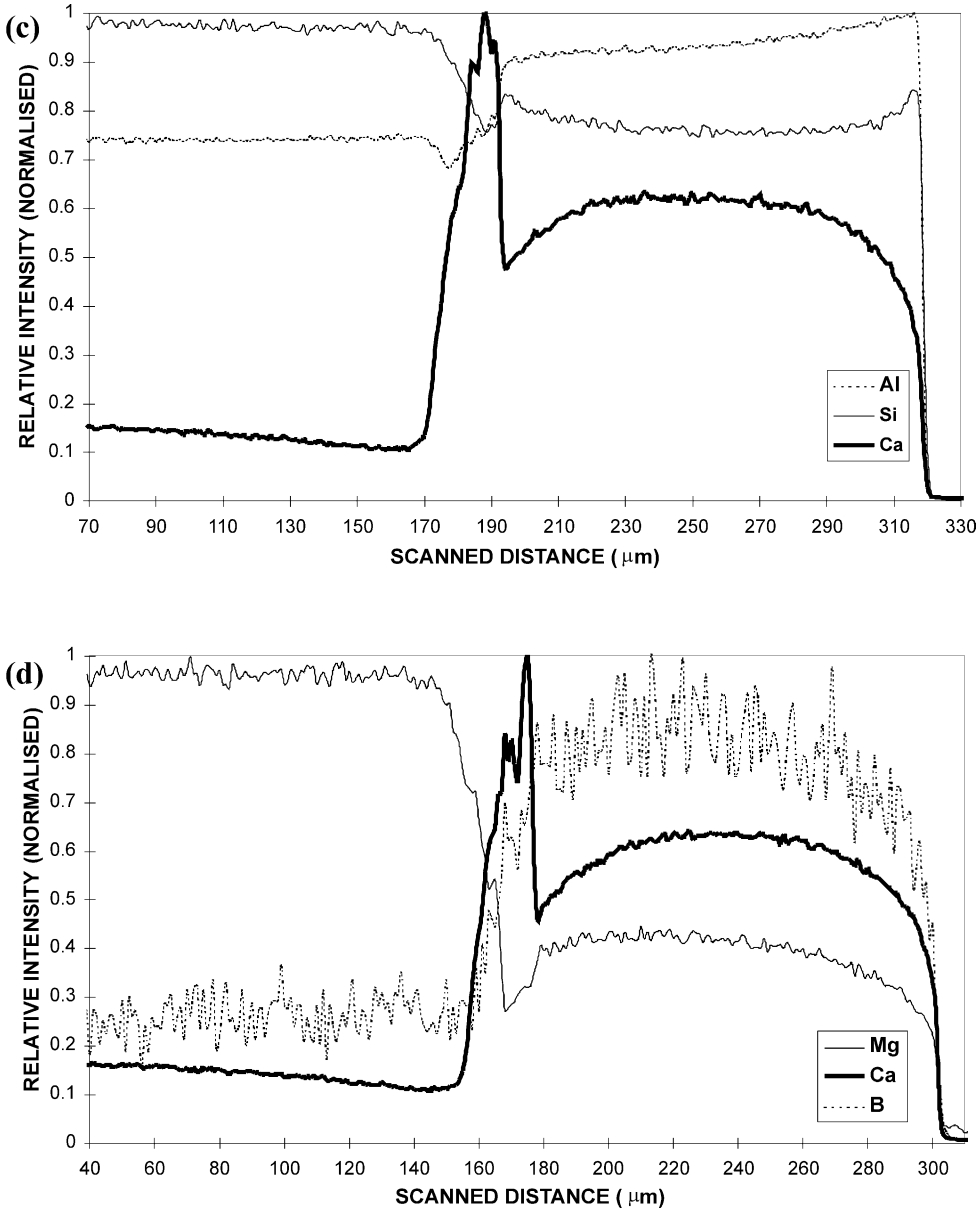

Fig. 4 (*continued*).

As can be seen, the profiles are rather complex, particularly across the interface region, due to the multi-layered character of the whole interaction layer, as was depicted previously by the SEM images of the same region for both glost firing temperatures (Fig. 1). The significant points to be observed in these profiles can be outlined as follows:

An intermediate layer whose Ca content is greater than that of either the adjacent glaze layer or of the body glass is clearly indicated at the interface. In addition, the Ca concentration both in the glaze and the glass is observed to decrease towards the interface, suggesting that the formation of this calcium rich layer was helped by the movement of Ca from the both directions. Another interesting observation is the behaviour of P at the interface. Firstly, its concentration decreases with a corresponding increase in the Ca concentration on the glass side of the interaction layer; it then increases and reaches a maximum with a further increase in the Ca concentration. Then, both the P and Ca concentration profiles show several peaks across the interaction layer followed by a sharp fall on the glaze side of the layer with no indication of solution into the glaze. Finally, a gradual drop in the Ca distribution profile towards the glaze surface is seen.

In the case of Na and K, there appears to be some degree of ion exchange taking place between Na in the glaze and K from the underlying body glass. This is shown by an increased amount of both Na and K at the interface. Na and K distribution profiles in the

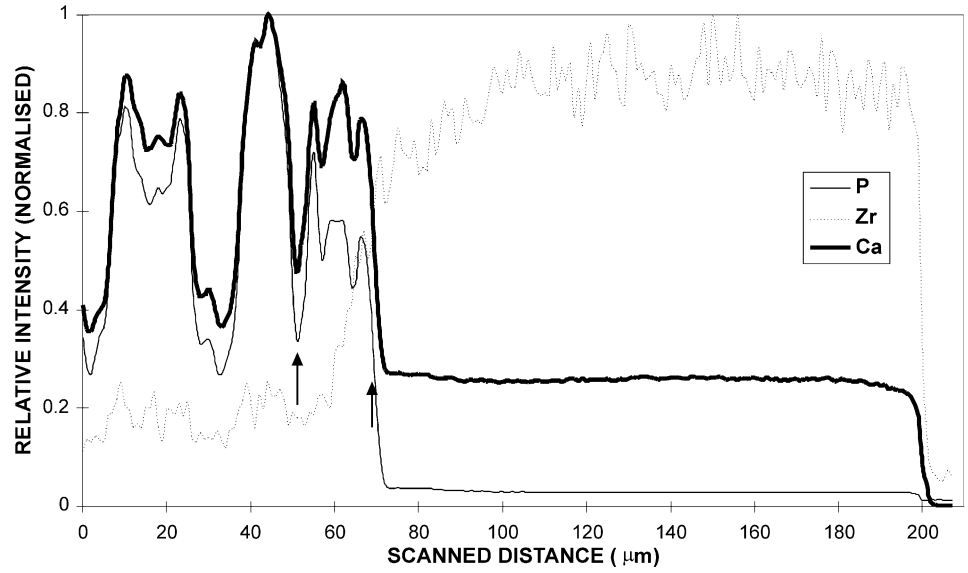

Fig. 5. The EPMA elemental distribution profiles across the ABS glaze–biscuit fired bone china body interface (glost fired at 1120 °C).

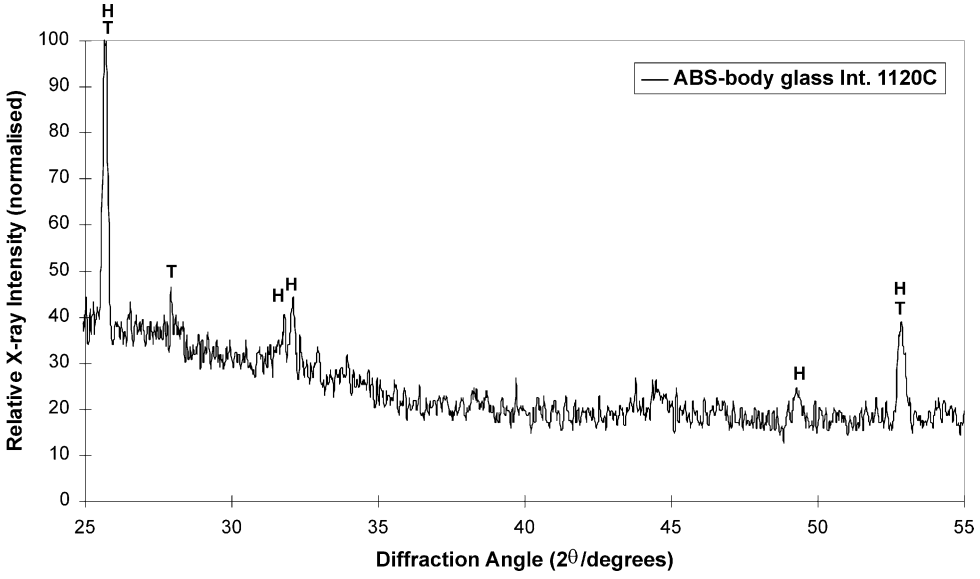

Fig. 6. A typical XRD spectrum of the ABS glaze–simulated bone china body glass interface (T: β-TCP, H: hydroxyapatite).

glaze layer exhibit a slight rise towards the glaze surface. The Si distribution profile is observed to be constant inside the body glass up to the point where there is a sudden rapid build up of Ca. Subsequently, it reduces to a minimum level through the Ca peak before showing an increase towards the glaze layer. The diffusion of Al into the body glass is also discernible with a gradual decrease of concentration across the interaction layer. Finally, the distribution profiles of the Si and Al inside the glaze layer present an increase towards the glaze surface. Zr and B elements diffuse from the glaze layer into the body glass through the interaction layer and reach a minimum level in the body glass. There is also a slight penetration of Mg from the body glass into the glaze but it is not present at the interface.

In order to show the preferential accumulation of Ca and P elements at the ABS glaze–biscuit fired bone china body interface EPMA was also employed. Fig. 5 illustrates such distribution profiles for Ca, P and Zr elements obtained across the interface. The interaction layer is marked with arrows on the figure verifying the presence of a calcium phosphate rich layer. Ca and P distribution profiles show further peaks inside the substrate due to the presence of β-TCP phase of the body. The presence of such a layer, consisting of aggregates of granular crystals, was shown by the earlier SEM studies in the second part of this study.[2] Regarding to

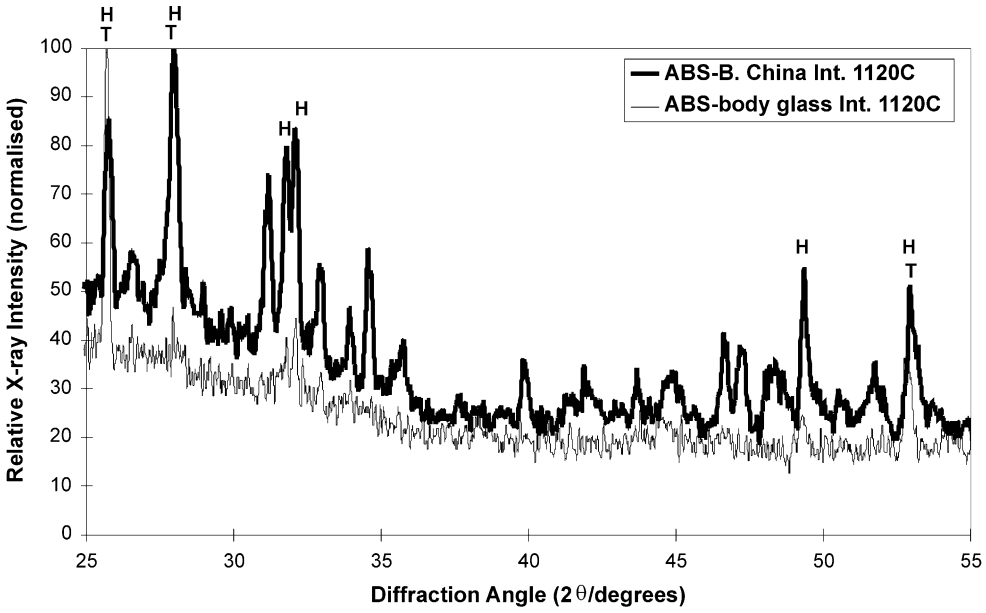

Fig. 7. A comparison of the XRD spectrum of the ABS glaze–simulated bone china body glass interface with that of the ABS glaze–biscuit fired bone china body interface (T: β-TCP, H: hydroxyapatite).

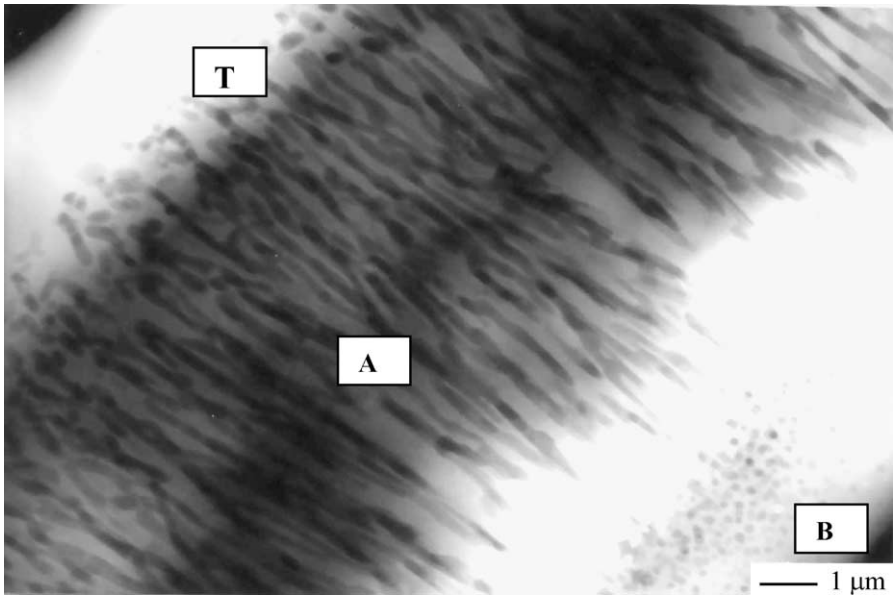

Fig. 8. A typical low magnification TEM image of the ABS glaze–simulated bone china body glass interface (glost fired at 1120 °C).

Zr, its concentration decreases over the interaction layer.

3.3. XRD results

Fig. 6 is a representative XRD spectrum of the ABS glaze-simulated bone china body glass interface glost fired at 1120 °C. There is a great deal of amorphous scattering on the spectra due to the amorphous nature of the glaze and the underlying glass substrate, overshadowing the characteristic peaks originating from the crystalline phases in the interaction layers formed at the interface. Comparison of the peaks on the XRD spectrum of the interface with standard reference patterns suggests that they are related to β-TCP (JCPDS-ICDD No: 09-169) and hydroxyapatite (JCDS-ICDD No: 09-432). The presence of hydroxyapatite was also noted in the interaction layers at the ABS glaze-biscuit fired bone china body interfaces in the second part of this study.[2] In addition, a comparison of the XRD spectrum of the ABS glaze-simulated bone china body glass interface with that of the ABS glaze–biscuit fired bone china body is illustrated in Fig. 7. As can be seen, the peaks from both interfaces correspond closely.

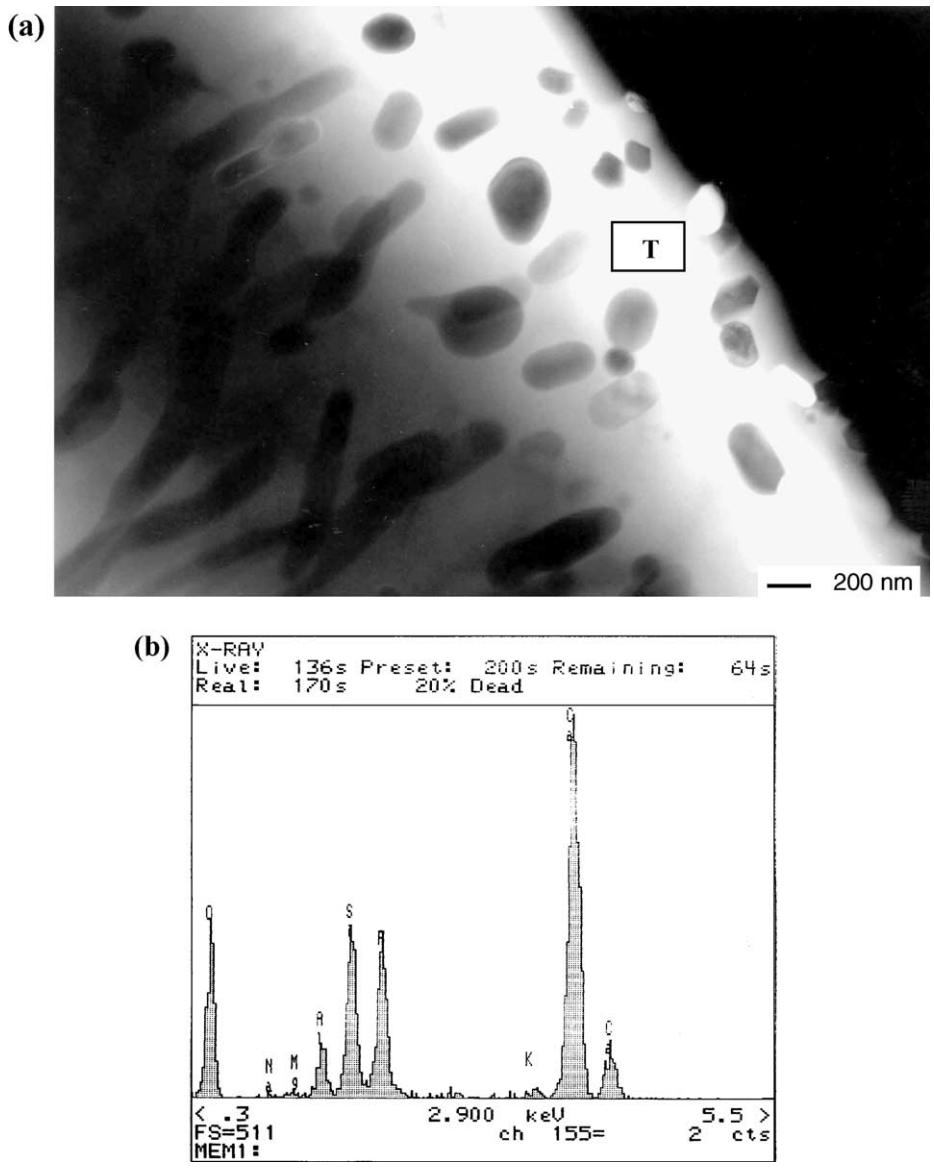

Fig. 9. (a) A typical TEM image of the granular crystals in layer T; (b) EDS spectrum of one of the granular crystals in layer T.

3.4. TEM results

Fig. 8 provides a typical view of the ABS glaze–simulated body glass interface, glost fired at 1120 °C, as revealed by TEM. It is a relatively low magnification image formed by displacing the objective aperture slightly in order to increase contrast. It shows the morphological features of the continuous interaction layers formerly designated as layer A and layer B (see Fig. 1). It is also evident that there is another interaction layer (marked as T), with a thickness of around 1 μm, formed directly on the acicular crystals in the layer A on the glaze side of the interface at this magnification. It appears to consist of single, granular crystals. The occurrence of this particular layer could not be detected from the relevant SEM images.

Fig. 9(a) is a TEM image of the layer T at higher magnification obtained by the slight displacement of the objective aperture. A number of granular crystals, of different sizes, distributed in a glassy phase can be clearly seen. EDS analyses carried out on these crystals revealed the presence of mainly Ca and P with varying amounts Si and Al. Such an EDS spectrum is shown in Fig. 9(b). The similar morphology and the chemistry of these crystals to the hydroxyapatite crystals at the ABS glaze–biscuit fired bone china body interface reported in the second part of this study is to be noted.[2]

Fig. 10(a) illustrates a bright field TEM image that was focused on the layer A. The acicular morphology and oriented growth of the crystals within the layer can be clearly seen. In addition, most of the crystals are

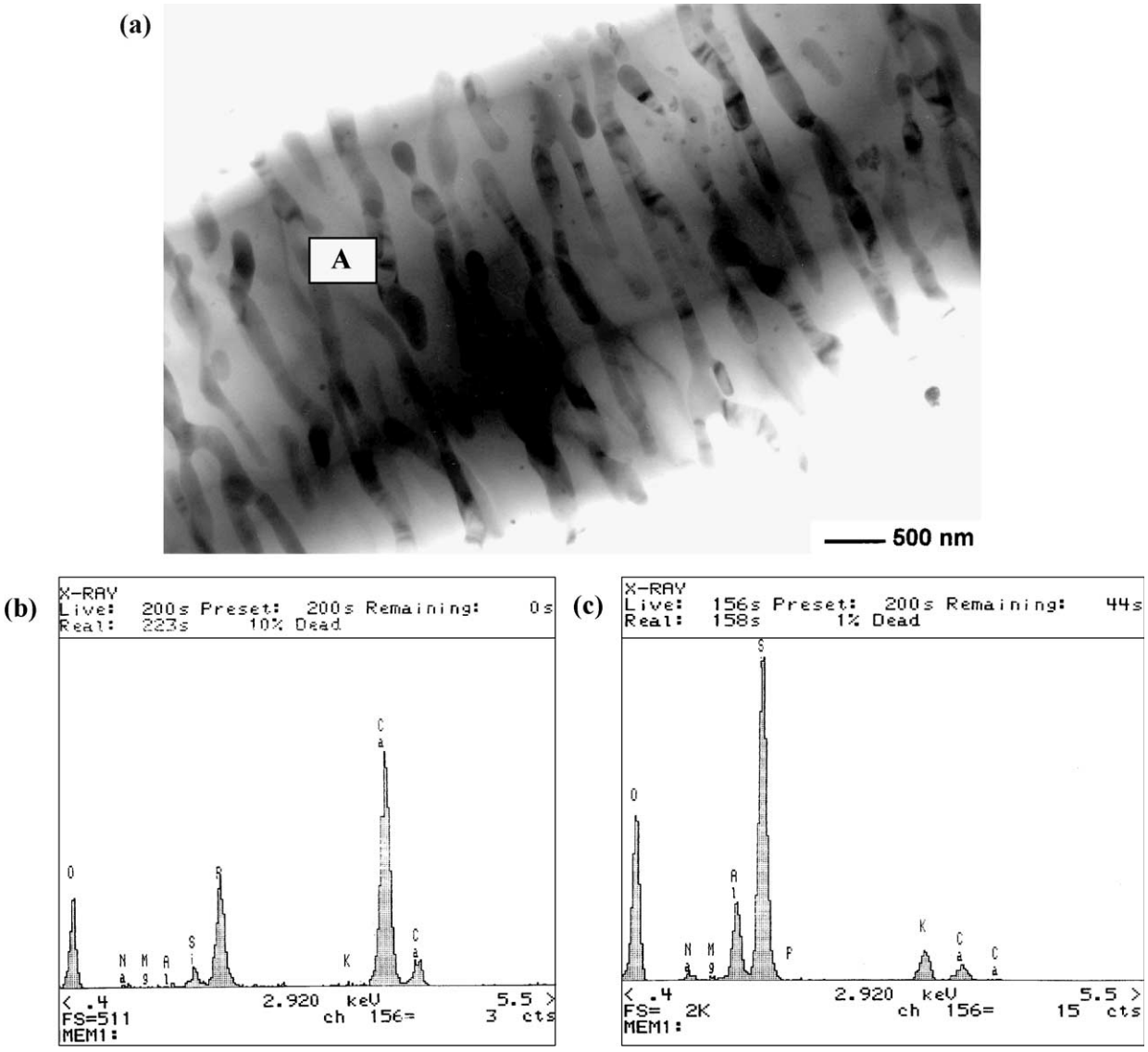

Fig. 10. (a) A typical bright field TEM image of the acicular crystals in layer A; (b) EDS spectrum of one of the acicular crystals in layer A; (c) EDS spectrum of the glassy phase between the acicular crystals in layer A.

observed to have branched. EDS analyses obtained from these crystals revealed high concentrations of Ca and P in their composition [Fig. 10(b)]. The glassy phase between the crystals was, however, found to be rich in mainly Si and Al. Of further interest is the lack of P in the glass [Fig. 10(c)].

A bright field TEM image is seen in Fig. 11(a), of the layer B that lies adjacent to the layer A on the glass substrate side of the interface. It is evident that the layer B consists of spherical crystals, with a diameter ranging from about 50 to 200 nm, embedded in a glassy matrix phase. EDS analyses on these crystals indicated the presence of high concentrations of Ca and P similar to the crystalline phases in both layer T and layer A. A typical EDS spectrum from a spherical crystal is presented in Fig. 11(b).

4. Conclusions

In regard to the contribution of the glassy matrix phase to the overall formation of the interaction layers at the ABS glaze–biscuit fired bone china body interface during glost firing, there appeared to be further indications that the formation of the hydroxyapatite crystals at the interface may be helped by its presence. These indications are summarized as below:

The formation of several continuous layers, consisting of glassy and crystalline phases with different morphology at the glaze–simulated body glass interfaces was observed by the electron microscopy techniques. The presence of Ca and P as major elements with different ratios in the crystalline phases was revealed in most cases. Of further interest was the morphological and

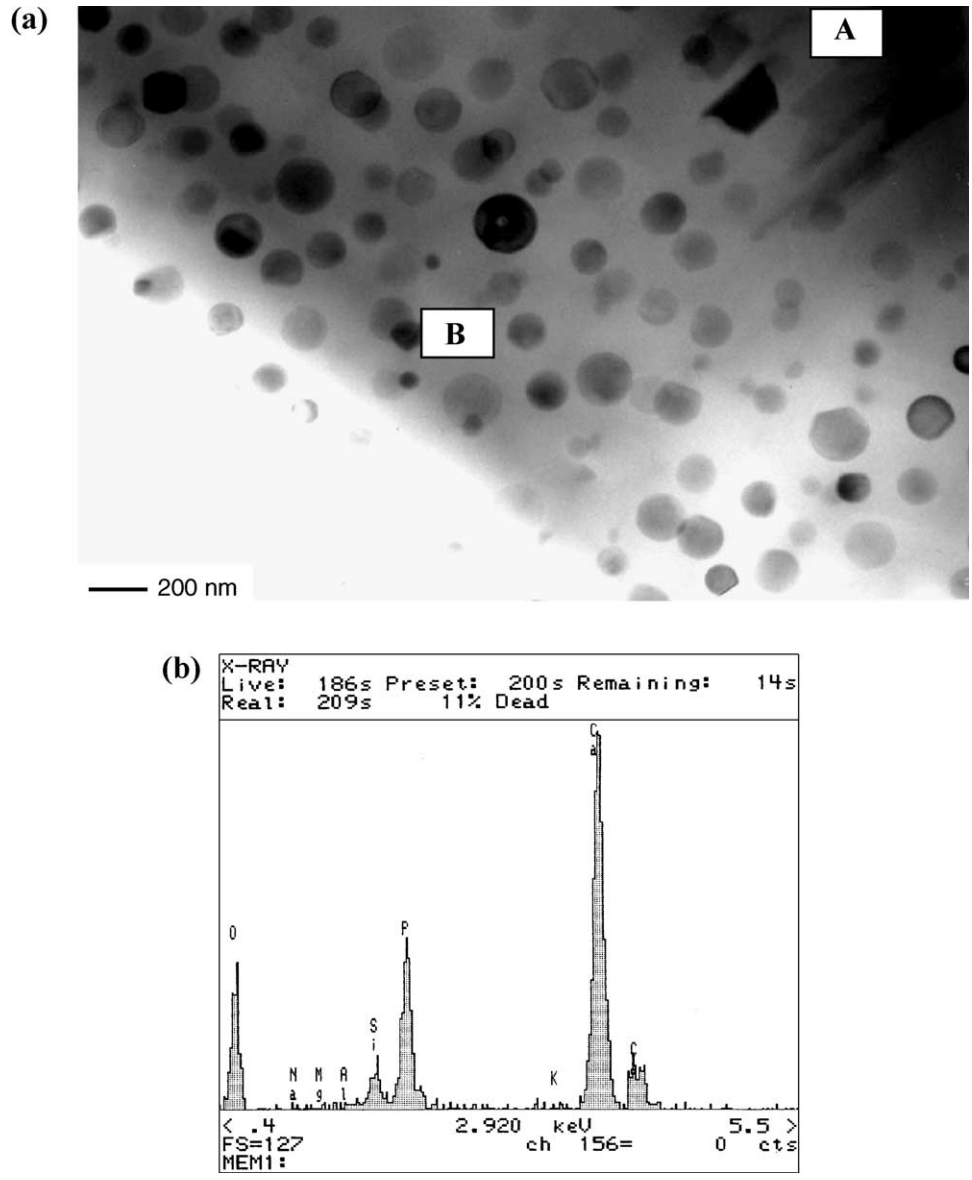

Fig. 11. (a) A typical bright field TEM image of the spherical crystals in layer B; (b) EDS spectrum of one of the spherical crystals in layer B.

chemical similarity of the granular crystals formed in the top layer, closest to the glaze layer at the glaze-simulated body glass interface (layer T), to the hydroxyapatite crystals at the glaze-biscuit fired bone china body interface illustrated in the second part of the study.[2] This may be also taken as implying participation of the glassy phase originally present in the biscuit fired bone china body in the formation of the interaction layers during glost firing. In regard to the acicular crystals, however, no such similarity could be reported. As a conclusion, it was suggested that the preferential reaction between P_2O_5 in the simulated glass and CaO in the glaze may well have resulted in the formation of these phases. No corresponding selected area diffraction (SAD) patterns were recorded, mainly due to unstable nature of the phases, becoming amorphous with the continued exposure to the electron beam.

The elemental distribution profiles acquired across the ABS glaze-simulated body glass interface glost fired at 1120 °C clearly demonstrated the complexity of the interaction layers involved in these systems. The presence of a calcium phosphate rich region, made up of several peaks of these elements with varying ratios, was demonstrated at the interface. In most cases, each peak is believed to correspond to an individual layer.

Both β-TCP and hydroxyapatite peaks appeared to be present on the representative XRD spectrum of the ABS glaze–simulated body glass interface. This can be taken as further evidence of a preferential reaction between P_2O_5 in the body glass originally present in the biscuit fired bone china body and CaO in the glaze at the interfaces, since phosphorus in varying amounts in the glassy phase was proved to be present by the TEM studies earlier.[4] This finding is significant since it indi-

cates that formation of the hydroxyapatite crystals at the ABS glaze–biscuit fired bone china body interface during glost firing may be helped by the rapid diffusion allowed by the glassy phase of the bone china body.

Due to the significant differences between the simulated glass and the original glassy phase, it is necessary to exercise caution when attempting to interpret the results given above. The relevant results are also inadequate to explain the exact mechanism whereby the calcium phosphate phases each having a distinct morphology occur.

Acknowledgements

The authors would like to thank the Anadolu University (Turkey) for the provision of a scholarship.

References

1. Kara, A. and Stevens, R., Interactions between an ABS type leadless glaze and a biscuit fired bone china body during glost firing—part I: preparation of experimental phases. *J. Eur. Ceram. Soc.*, 2002, **22**(7), 1095–1102.
2. Kara, A. and Stevens, R., Interactions between an ABS type leadless glaze and a biscuit fired bone china body during glost firing—Part II: investigation of interactions. *J. Eur. Ceram. Soc.*, 2002, **22**(7), 1103–1112.
3. Kara, A. and Stevens, R., Characterisation of biscuit fired bone china body microstructure—Part I: XRD and SEM of Crystalline Phases. *J. Eur. Ceram. Soc.*, 2002, **22**(5), 731–736.
4. Kara, A. and Stevens, R., Characterisation of biscuit fired bone china body microstructure—Part II: transmission electron microscopy (TEM) of glassy matrix. *J. Eur. Ceram. Soc.*, 2002, **22**(5), 737–743.
5. Roberts, G. J and Beech, D. G., *Some Effects of Firing-schedule on the Translucency and Porosity of Bone China.* Research Paper No. 296, Br. Ceram. Res. Assoc., 1951.
6. Iqbal, Y., Messer, P. F. and Lee, W. E., Non-equilibrium microstructure of bone china. *Br. Ceram. Trans.*, 2000, **993**, 110–116.
7. Iqbal, Y., Messer, P. F. and Lee, W. E., Microstructural evolution in bone china. *Br. Ceram. Trans.*, 2002, **995**, 193–199.
8. Ruddlesden, S. N. and Airey, A. C., Applications of the electron probe microanalyser to ceramics III. General research problems. *Trans. Br. Ceram. Soc.*, 1967, **66**, 607–629.
9. Roberts, W. and Marshall, K., Glaze-body reactions: electrochemical studies. *Trans. Br. Ceram. Soc.*, 1970, **69**(6), 221–241.
10. Newcomb, S. B., Boothroyd, C. B. and Stobbs, W. M., Specimen preparation methods for the examination of surfaces and interfaces in the transmission electron microscope. *J. Microscopy*, 1985, **140**(2), 195–207.
11. Ruddlesden, S.N., *The Application of Electron Probe Microanalysis to Textural Studies of Ceramics*, Res. Pap. No. 632, Br. Ceram. Res. Assoc., 1971.
12. Engelke, H., Property changes at interfaces and free surfaces. In *Surfaces and Interfaces of Glass and Ceramics. Materials Science Research, Vol. 7*, ed. V. D. Frechette, W. C. LaCourse and V. L. Burdick. Plenum Press, New York, 1974, pp. 411–425.
13. Whitney, W. P., Electron microprobe analysis of glaze/glass-ceramic interface reactions. *J. Non-Crystalline Solids*, 1980, **38–39**, 687–692.
14. Ribbe, P. H. and Smith, J. V., X-ray emission microanalysis of rock-forming minerals IV. Plagioclase Feldspars. *J. Geol.*, 1966, **74**, 217–233.
15. Ohuchi, F. and Holloway, P. H., General model of sodium desorption and diffusion during electron bombardment of glass. *J. Vac. Sci. Technol.*, 1982, **20**(3), 863–867.
16. Borom, M. P. and Hanneman, R. E., Local compositional changes in alkali silicate glasses during electron microprobe analysis. *J. Appl. Phys.*, 1967, **38**(5), 2406–2407.
17. Lineweaver, J. L., Oxygen outgassing caused by electron bombardment of glass. *J. Appl. Phys.*, 1963, **346**, 1786–1791.
18. Varshneya, A. K., Cooper, A. R. and Cable, M., Changes in composition during electron micro-probe analysis of K_2O-SrO-SiO_2 glass. *J. Appl. Phys.*, 1966, **37**(5), 2199.
19. Vassamillet, L. F. and Caldwell, V. E., Electron-probe microanalysis of alkali metals in glasses. *J. Appl. Phys.*, 1969, **404**, 1637–1643.
20. Kane, W. T., Applications of the electron microprobe in ceramics and glass technology. In *Microprobe analysis*, ed. C. A. Anderson. John Wiley & Sons, New York, 1973, pp. 241–270.